# Bayesian Approach for Network Modeling of Brain Structural Features

Anand A. Joshi[a], Shantanu H. Joshi[a], Richard M. Leahy[b], David W. Shattuck[a], Ivo Dinov[a] and Arthur W. Toga[a]

[a]Laboratory of Neuro Imaging, University of California, Los Angeles, CA 90095-7334, USA; [b]Signal and Image Processing Institute, University of Southern California, Los Angeles, CA 90089-2564, USA

## ABSTRACT

Brain connectivity patterns are useful in understanding brain function and organization. Anatomical brain connectivity is largely determined using the physical synaptic connections between neurons. In contrast statistical brain connectivity in a given brain population refers to the interaction and interdependencies of statistics of multitudes of brain features including cortical area, volume, thickness etc. Traditionally, this dependence has been studied by statistical correlations of cortical features. In this paper, we propose the use of Bayesian network modeling for inferring statistical brain connectivity patterns that relate to causal (directed) as well as non-causal (undirected) relationships between cortical surface areas. We argue that for multivariate cortical data, the Bayesian model provides for a more accurate representation by removing the effect of confounding correlations that get introduced due to canonical dependence between the data. Results are presented for a population of 466 brains, where a SEM (structural equation modeling) approach is used to generate a Bayesian network model, as well as a dependency graph for the joint distribution of cortical areas.

**Keywords:** Bayesian Networks, structural equation modeling, structure learning, cortical features

## 1. INTRODUCTION

Human brains are known to be organized in a large-scale network formed by neurons (basic units that store, process and transmit information) and their specialized interconnections (synapses). This brain network is massively complex, hierarchical and can be decomposed and studied at different scales for easier understanding. Brain connectivity refers to a pattern of anatomical links (anatomical connectivity), of statistical dependencies (functional connectivity) or causal interactions (effective connectivity) between distinct units of the brain. The connectivity patterns are either determined by directly observing structural links such as synapses or fiber pathways, or by representing statistical or causal relationships measured as cross-correlations, coherence, or information flow. More specifically, brain network analysis has been traditionally performed at several levels, viz. i) cellular level,[1] ii) macroscopic aggregated level[2,3] (using structural connectivity information such as DTI), and the iii) functional level[4–7] (using functional data such as fMRI and EEG). Each of these approaches study brain connectivity via diverse anatomical and functional characteristics of the brain, and are extremely helpful in determining both local and global, as well as low-level, and high-level architectural and functional organization of the brain. However, the structural networks of the human cerebral cortex have not yet been comprehensively mapped,[8] and much work remains to be done. Apart from the physical neuronal connections, the cerebral cortex is shown to consist of clusters of densely and reciprocally coupled globally interconnected cortical regions. Of late, researchers have started exploiting this knowledge in order to determine statistical brain connectivity patterns in populations. These approaches also termed as "effective networks",[9] are beginning to be useful for determining structural networks based on morphological properties such as cortical thickness, areas, and volumes are receiving renewed attention for the purpose of understanding the organizational principles in the human brain. Analyses of structural brain connectivity patterns, for example of large-scale connectivity matrices of the cerebral cortex, allow the quantification of a broad range of network characteristics.[10] Sporns et al.[8] have

Further author information: (Send correspondence to Anand A. Joshi)
Anand A. Joshi: E-mail: anand.joshi@loni.ucla.edu

Medical Imaging 2010: Biomedical Applications in Molecular, Structural, and Functional Imaging, edited by Robert C. Molthen, John B. Weaver, Proc. of SPIE Vol. 7626, 762607 · © 2010 SPIE
CCC code: 1605-7422/10/$18 · doi: 10.1117/12.844548

referred to the connectivity matrix as the human connectome and have proposed a comprehensive approach for its construction. A similar idea has been used by[11] for understanding the functional brain states associated with their structural counterparts. Friston et al.[12] also use dynamic causal modeling in order to estimate and make inferences about directed dependencies between variables. Large-scale cortical networks share some attributes of small-world networks, including high values for clustering coefficients and short characteristic path lengths, and they are composed of specific sets of structural motifs.[13] An analysis of the structural contributions of individual areas allows the identification and classification of network centers, defined as highly connected and highly central brain regions, which include areas of parietal and prefrontal cortex. Structural networks based on morphological properties such as cortical thickness has received attention in order to understand structural organizational principles in the human brain can enhance our understanding of how functional brain states are associated with their structural substrates.

Our goal is to model inter-dependencies between different brain structures. These relationships may be either causal (i.e. changes in a given specific type of a brain sub-structure are a direct consequence of changes in another type of a sub-structure), or correlated. In either case, the relationships are usually inferred statistically from the observed data. Furthermore these relationships can be conveniently represented by networks or graphs, where the nodes of such graphs are random variables corresponding to the observed data values. Examples of graphical models[14] include Markov random fields and Bayesian networks.[15] Markov random fields encode undirected graphs, whereas Bayesian networks assign directionality to each of the links of the graph. Both of these approaches involve the introduction of a set of unobserved, "hidden" variables that simplify the model. Yet other approaches[?] have constructed networks that only depend upon the estimated correlation coefficients between the observed data. Formally, Bayesian networks are directed acyclic graphs whose nodes represent random variables in the Bayesian sense: they may be observable quantities, latent variables, unknown parameters or hypotheses. Edges represent conditional dependencies; nodes which are not connected represent variables which are conditionally independent of each other. Each node is associated with a probability function that takes as input a particular set of values for the node's parent variables and gives the probability of the variable represented by the node. The Bayesian network then represents a set of random variables and their conditional independences via a directed acyclic graph (DAG). For example, a Bayesian network could represent the probabilistic relationships between diseases and symptoms. Given a set of symptoms, the network can be used to compute the probabilities of the presence of various diseases.

Automatically learning the graph structure of a Bayesian network is a challenge pursued within machine learning. The basic idea goes back to a recovery algorithm developed by Rebane and Pearl[16] and rests on the distinction between the three possible types of adjacent triplets allowed in a directed acyclic graph. In this paper, we focus on a Bayesian network modeling approach for estimating statistical dependencies of surface areas of cortical hemispheric sub-regions with respect to each other. These dependencies will be further used for learning and modeling brain structure networks. In our application the underlying network structure is assumed to be unknown. In this case the network structure and the parameters of the local distributions must be learned from imaging data. We achieve this by deriving the joint probability distribution of the cortical area, and succinctly represent and visualize them by a partially directed graph. This graph representation of joint distribution can help in understanding causal as well as correlational relationships across regions. We propose a new approach for obtaining the connectivity in brain regions based on Bayesian networks rather than simple correlation coefficients. More specifically, we use structural equation approach for modeling the joint distribution of parcellated cortical areas. The mechanisms of brain networks at at a higher level, can be conveniently represented and studied under a graph-theoretic framework. Throughout this paper, graphical models will be considered at the macroscopic level, where the vertices of graphs represent individual anatomical regions, and the edges denote the connectivity relationships between them. As a fundamental and intuitive tool to analyze and visualize the association and/or causality relationships among multiple events, graphical models have become more and more common in biomedical researches, such as discovering gene regulatory networks and modeling functional connectivity between brain regions. In these real world applications, graphical models are not only a tool for operations such as classification or prediction, but often the network structures of the models themselves are also output of great interest: a set of association and/or causality relationships discovered from experimental observations. We describe our approach for obtaining the network structure in the following sections.

## 2. METHODS

This section highlights the main algorithm in the paper. In this paper, we focus on cortical surface area obtained from the gray matter (GM) measurements, although in the future surface characteristics such as curvature for cortical regions, and even additional measurements such as diffusion tensor data can be included. We also currently omit subcortical regions such as the hippocampus, caudate etc. and only concentrate on the surface measures. In the following subsections, we describe the steps and procedures, leading from the collection and processing of brain MRI data, segmentation of cortical structures, as well as modeling the joint distributions of the parcellated cortical areas leading to the construction of the brain connectivity map using Bayesian networks.

### 2.1 Data collection and preprocessing

The data consists of 3D structural brain MRI scans of 466 normal right handed subjects (age range: $22-25$ years). The scans were collected using a 4 Tesla Bruker Medspec whole body scanner (Bruker Medical, Ettingen, Germany) at the Center for Magnetic Resonance (University of Queensland, Australia). Three-dimensional $T1$-weighted images were acquired with a magnetization prepared rapid gradient echo ($MP\text{-}RAGE$) sequence to resolve anatomy at high resolution. Acquisition parameters were: inversion time ($TI$) /repetition time ($TR$) /echo time ($TE$) = 1500 / 2500 / 3.83 $msec$; flip angle = $15^o$; slice thickness = 0.9 $mm$ with a 256x256x256 acquisition matrix. In this paper, we used parcellation of grey matter volume as our structural data. In order to get structural data statistics, we used Freesurfer's automated processing pipeline for automatic skull stripping, tissue classification, surface extraction, cortical and subcortical parcellations. It calculates volumes of individual grey matter parcellations in $mm^3$ and surface area in $mm^2$. Additionally it also provides surface and volume statistics for about 34 different cortical structures, and also computes geometric characteristics such as curvature, curvedness, local foldedness for each of the parcellations. In this work, we used cortical areas as anatomical features to find the structural connectivity. Figure 1 shows the lateral, frontal, and medial views of the cortex parcellated and color coded into 34 regions.

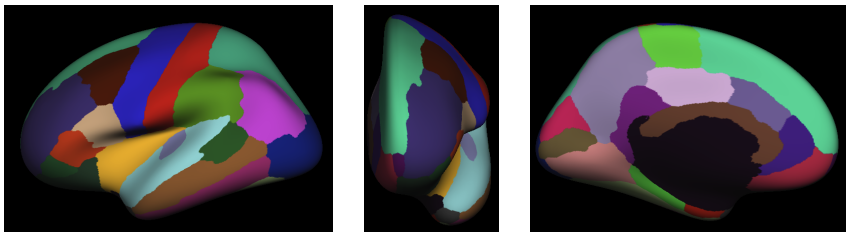

Figure 1. Lateral, frontal, and medial views of the cortex parcellated into 34 regions.

### 2.2 Analysis of distributions of segmented measurements

After segmenting the cortical areas, we tried to ascertain the distribution of the surface area across the population. An initial view of the distribution of the gray matter volumes revealed non-Gaussian properties. Figure 2 shows histograms of gray matter volumes corresponding to all 34 regions for total number of 466 subjects. It was observed that a log normal distribution with parameters $(\mu, \sigma)$ given by the form $p(x) = \frac{1}{x\sigma\sqrt{2\pi}} \exp \frac{(\log x - \mu)^2}{2\sigma^2}$ fitted the observed data quite well. To perform quantitative validation of log-normality, we performed a log transformation on this data and performed Lilliefors test[17] on the transformed data to check for normality. The test was passed, thus validating the lognormal assumption. The subsequent analysis and construction of the networks was performed by computing the logarithm of the measurements so as to transform the gray-matter volume data to have a multivariate normal distribution.

### 2.3 Bayesian Network Extraction from Structural equation Modeling

Structural equation models (SEMs) provide a general framework for modeling implicit relationships in multivariate random variables.[18–20] Although SEMs are most commonly used in studies involving intrinsically latent variables, such as happiness, quality of life, or stress, they also provide a parsimonious framework for covariance

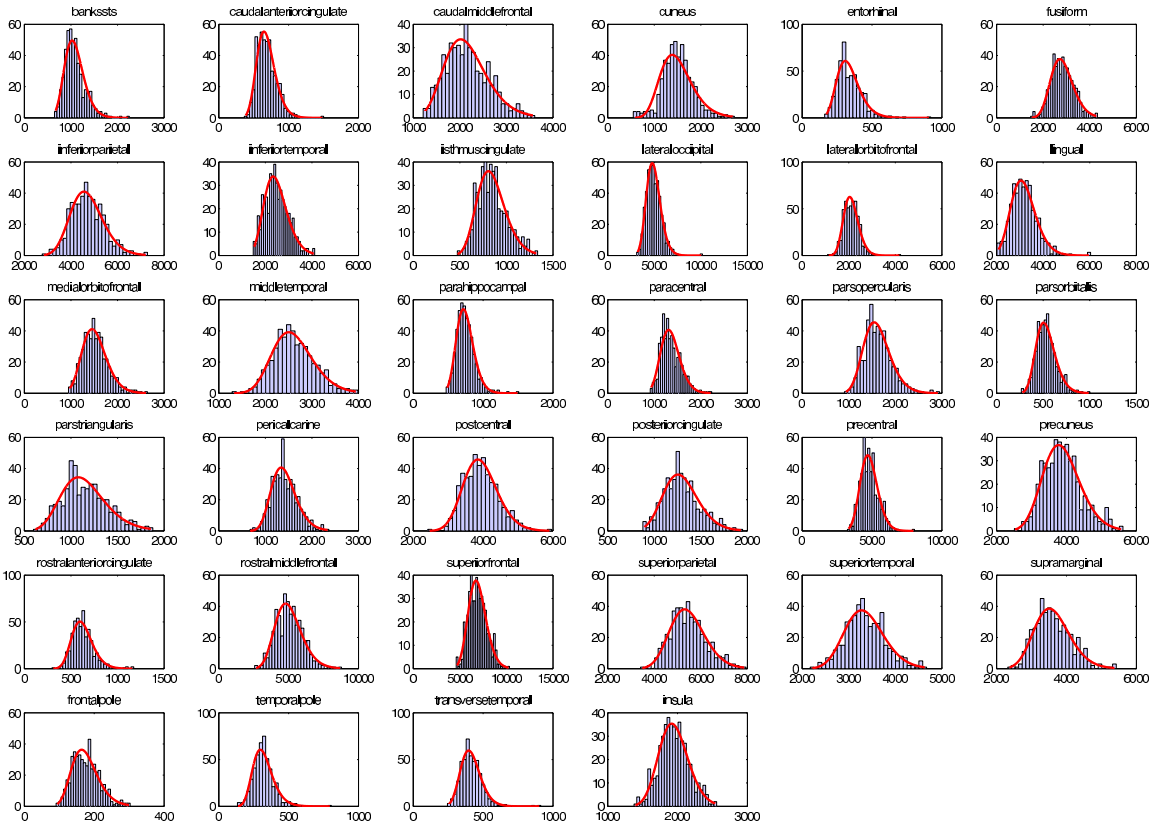


Figure 2. Histograms of surface areas for 34 labeled region, with the fitted Log-normal distributions overlaid in red.

structure modeling.[21] For this reason, they have become increasingly used outside of the traditional social science applications. Additionally, the SEM graph also provides causal and correlational dependence between these variables which can help in understanding various network properties of different areas. For example, one can answer questions such as, which cortical regions are central to development and how they influence development of other cortical regions in the brain. The SEM graph extracted from this data can provide insight into interdependence between these variable and help in understanding development of brain. In pathological cases, such as Alzheimer's disease, one can study causal and correlational structure of disease propagation using this network, although in this paper, we only considered a population of normal brains.

As discussed in Sec. 2.2, the input to the SEM algorithm was the log-transformed data of surface areas of different brain regions. Next, we followed a two step procedure to extract the SEM graph structure of the data, viz. i) Structural Equation Modeling (SEM) Skeleton Extraction, and ii) SEM parametric model estimation. These steps are implemented in Tetrad IV software by Spirtes et al.,[22] available from `http://www.phil.cmu.edu/projects/tetrad/index.html` .

### 2.3.1 SEM Skeleton Estimation

We use the PC skeleton algorithm **??** for determining the skeleton of the desired SEM graph. The PC skeleton algorithm is designed to search for causal explanations of observational data in which it may be assumed that the true causal hypothesis is acyclic in nature. We outline the algorithm below, but refer the reader to[23,24] for detailed description and explanation. The algorithm operates by asking a conditional independence oracle to make judgments about the independence of pairs of variables (e.g., $X$, $Z$) conditioned on sets of variables (e.g., $\{Y\}$). Conditional independence test between a pair of variables from a multivariate Gaussian is performed by computing partial correlation between the two variables, controlling the conditioned variables. The adjacency

graph structure is extracted in the algorithm by constructing a complete undirected graph over the variables and then removing the edges $X - Y$ if some set $S$ among either the adjacent of $X$ or $Y$ can be found such that $X$ and $Y$ are conditionally independent given $S$. After the graph is constructed, the SEM parametric model is estimated from the skeleton by PC algorithm.

### 2.3.2 SEM parametric model

Each variable representing cortical area of a parcellation is represented as a linear sum of its parents plus an exogenous error term–e.g., $X_1 = a_1(X_2) + a_2(X_3) + e_1$, $X_2 = a_3(X_3) + e_2$, and so on, where the distribution of each error terms has a specified variance and correlations among error terms are specified. The graph for such a system consists of one node for each variable, one node for each error term, a directed edge from each variable on the right hand side each such equation above to the variable on the left hand side of the equation. In other words, a directed edge represents a causal relationship between the pair of variables. The bidirected edges between each pair of variables denote variables with correlated error terms. The parameters in this model consist of:

1. Linear coefficients in the structural equations (e.g., $a_1$, $a_2$, and $a_3$, above),
2. Variances of each error term(e.g., var($e_1$), var($e_2$), above),
3. Covariances of each pair of correlated error terms.

The above parameters are estimated using the maximum likelihood parameter estimation[23, 25] from the surface areas of different regions. The estimated parameters are represented pictorially as well as in a tabulated format in Sec. 3.

## 3. EXPERIMENTAL RESULTS

Figure 3 shows the Bayesian network obtained from the application of PC algorithm to the surface area data corresponding to 34 cortical regions for the population of 466 brains. For a better visualization of brain connectivity, we have shown network edges overlaid on a flattened representation of the cortex. The flattened map was generated by Freesurfer, and follows same labeling and color coding scheme of the original parcellated surface shown in Fig. 1. We only display the causal connections (unidirected) between brain regions. We can observe both short-range and long-range causal connectivity relationships across regions. The SEM model yields a set of equations representing joint distribution of the variables. For example, $X_i = a_1X_1 + a_2X_2 + ... + e_i$. The coefficients, $a_1, a_2$ etc are denoted as directed arrows $X_1 \rightarrow X_i$, $X_2 \rightarrow X_i$, etc with those weights. These are shown in Fig. 3. The mean and standard deviations of the error terms $e_i$s are tabulated in Table 1, whereas the covariances between the error terms are pictorially depicted in Fig. 4. We note that there is some degree of left-right symmetry in connections with large weights but we also observed asymmetry in some connections. This will be explored further.

## 4. CONCLUSION AND DISCUSSION

The parametric description for the joint distribution of the cortical sheet presented in this paper can be helpful in understanding causal and correlated dependencies between descriptive features of brain regions. Although we use surface area as the cortical feature in this work, one can also use other features such as volumes, thickness, or any other descriptive features that can be anatomically measured on the cortical sheet. In the future, this representation can be helpful in a richer understanding of the functional associations and interdependencies of different regions. This compact representation of the joint distribution of the cortical sheet can be helpful in understanding normal as well as abnormal brain development. Using these graph models, one can analyze the redistribution/reconfiguration of cortical sheet for specialized cases, such as blind, hearing impaired populations. We plan to conduct these studies in the future.

Table 1. Error statistics for the SEM model for each of the 34 regions for both left and right hemispheres. The 34 regions are labeled according to Freesurfer. For each hemisphere, the mean and the standard deviation of the estimated error is shown.

| **No.** | **Cortical Region** | **Left** | | **Right** | |
|---|---|---|---|---|---|
| | | **Mean** | **Std Deviation** | **Mean** | **Std Deviation** |
| 1 | bankssts | 6.9708 | 0.1507 | 6.6905 | 0.218 |
| 2 | caudalanteriorcingulate | 6.5109 | 0.1478 | 6.5073 | 0.1795 |
| 3 | caudalmiddlefrontal | 7.6572 | 0.216 | 7.7013 | 0.1981 |
| 4 | cuneus | 7.2909 | 0.2354 | 7.246 | 0.1507 |
| 5 | entorhinal | 5.7917 | 0.2362 | 5.8209 | 0.2389 |
| 6 | fusiform | 7.9383 | 0.1409 | 7.9252 | 0.1595 |
| 7 | inferiorparietal | 8.4476 | 0.1505 | 8.4808 | 0.1424 |
| 8 | inferiortemporal | 7.798 | 0.1487 | 7.7693 | 0.1876 |
| 9 | isthmuscingulate | 6.7267 | 0.1528 | 6.7059 | 0.1407 |
| 10 | lateraloccipital | 8.4973 | 0.1545 | 8.4157 | 0.1459 |
| 11 | lateralorbitofrontal | 7.6453 | 0.1138 | 7.7029 | 0.1327 |
| 12 | lingual | 8.0515 | 0.1497 | 7.9821 | 0.1189 |
| 13 | medialorbitofrontal | 7.3118 | 0.175 | 7.3233 | 0.1654 |
| 14 | middletemporal | 7.8546 | 0.1701 | 7.8994 | 0.1433 |
| 15 | parahippocampal | 6.6033 | 0.1539 | 6.5806 | 0.1372 |
| 16 | paracentral | 7.2007 | 0.1345 | 7.3842 | 0.1296 |
| 17 | parsopercularis | 7.376 | 0.1543 | 7.2557 | 0.1631 |
| 18 | parsorbitalis | 6.2633 | 0.197 | 6.5927 | 0.1394 |
| 19 | parstriangularis | 7.029 | 0.1614 | 7.288 | 0.1525 |
| 20 | pericalcarine | 7.2368 | 0.1595 | 7.2329 | 0.1746 |
| 21 | postcentral | 8.2715 | 0.084 | 8.3208 | 0.1053 |
| 22 | posteriorcingulate | 7.156 | 0.1322 | 7.0956 | 0.1273 |
| 23 | precentral | 8.4716 | 0.0901 | 8.494 | 0.0922 |
| 24 | precuneus | 8.2557 | 0.1396 | 8.2541 | 0.1041 |
| 25 | rostralanteriorcingulate | 6.4248 | 0.1592 | 6.3141 | 0.2057 |
| 26 | rostralmiddlefrontal | 8.5105 | 0.1229 | 8.5698 | 0.1248 |
| 27 | superiorfrontal | 8.8332 | 0.0893 | 8.8028 | 0.0755 |
| 28 | superiorparietal | 8.5963 | 0.1397 | 8.5427 | 0.1023 |
| 29 | superiortemporal | 8.1105 | 0.1273 | 8.1369 | 0.1196 |
| 30 | supramarginal | 8.1835 | 0.1428 | 8.2734 | 0.1555 |
| 31 | frontalpole | 5.1479 | 0.217 | 5.4888 | 0.2075 |
| 32 | temporalpole | 5.7475 | 0.2178 | 5.734 | 0.2066 |
| 33 | transversetemporal | 6.0129 | 0.1404 | 5.9332 | 0.2194 |
| 34 | insula | 7.5706 | 0.0732 | 7.5963 | 0.1138 |

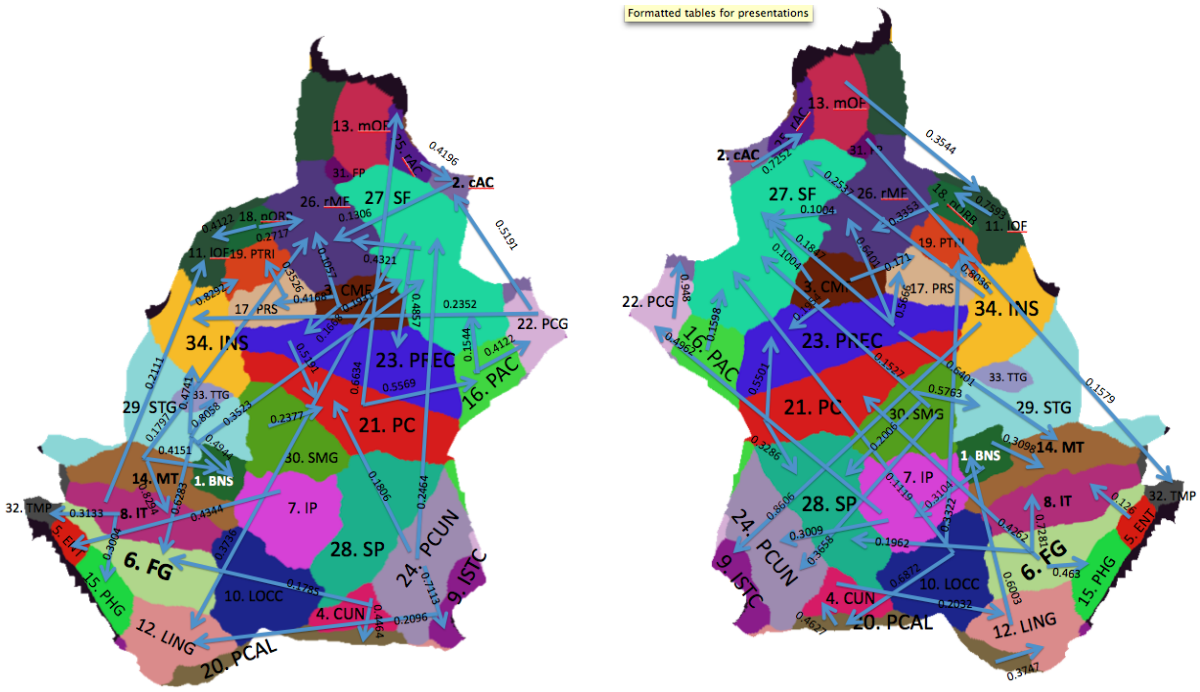


Left Hemisphere Right Hemisphere

Figure 3. Causal connections between 34 labeled regions along with their weights displayed on a flattened representation of the cortex for both left and right hemispheres.

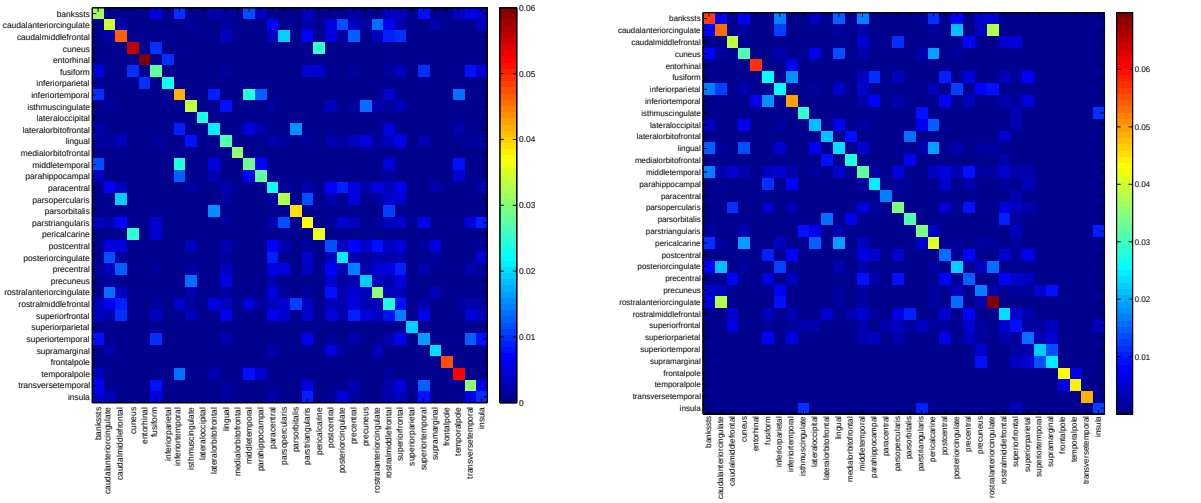


Figure 4. Error covariances of the SEM model for both left and right hemispheres.

## ACKNOWLEDGMENTS

This research was partially supported by the National Institute of Health through the NIH Roadmap for Medical Research, Grant U54 RR021813.

## REFERENCES


[1] Hashemi, M., Buibas, M., and Silva, G. A., "Automated detection of intercellular signaling in astrocyte networks using the converging squares algorithm," *Journal of Neuroscience Methods* **170**(2), 294 – 299 (2008).

[2] Hagmann, P., Kurant, M., Gigandet, X., Thiran, P., Wedeen, V. J., Meuli, R., and Thiran, J.-P., "Mapping human whole-brain structural networks with diffusion mri," *PLoS ONE* **2**(7), e597 (2007).

[3] Gong, G., He, Y., Concha, L., Lebel, C., Gross, D. W., Evans, A. C., and Beaulieu, C., "Mapping Anatomical Connectivity Patterns of Human Cerebral Cortex Using In Vivo Diffusion Tensor Imaging Tractography," *Cereb. Cortex* **19**(3), 524–536 (2009).

[4] Salvador, R., Suckling, J., Coleman, M. R., Pickard, J. D., Menon, D., and Bullmore, E., "Neurophysiological Architecture of Functional Magnetic Resonance Images of Human Brain," *Cereb. Cortex* **15**(9), 1332–1342 (2005).

[5] Achard, S., Salvador, R., Whitcher, B., Suckling, J., and Bullmore, E., "A Resilient, Low-Frequency, Small-World Human Brain Functional Network with Highly Connected Association Cortical Hubs," *J. Neurosci.* **26**(1), 63–72 (2006).

[6] Friston, K. J., "Functional and effective connectivity in neuroimaging: a synthesis," *Human Brain Mapping* **2**(2), 56–78 (1994).

[7] Friston, K., [*Functional connectivity*], Academic Press, 2nd ed. (2003).

[8] Sporns, O., Tononi, G., and Kotter, R., "The human connectome: a structural description of the human brain," *PLoS Comput Biol* **1**(4), e42 (2005).

[9] Honey, C. J., Ktter, R., Breakspear, M., and Sporns, O., "Network structure of cerebral cortex shapes functional connectivity on multiple time scales," *Proceedings of the National Academy of Sciences* **104**(24), 10240–10245 (2007).

[10] Sporns, O. and Zwi, J., "The small world of the cerebral cortex," *Neuroinformatics* **2**(2), 145–162 (2004).

[11] He, Y., Chen, Z. J., and Evans, A. C., "Small-World Anatomical Networks in the Human Brain Revealed by Cortical Thickness from MRI," *Cereb. Cortex* **17**(10), 2407–2419 (2007).

[12] Friston, K., [*Dynamic Causal Models*], Academic Press, 2nd ed. (2003).

[13] Sporns, O. and Ktter, R., "Motifs in brain networks," *PLoS Biol* **2**, e369 (10 2004).

[14] Lauritzen, S. L., "Graphical models," Clarendon Press, Oxford University Press (1996).

[15] Pearl, J., "Probabilistic reasoning in intelligent systems," Mogan Kaufmann (1988).

[16] Rebane, G. and Pearl, J., "The recovery of causal poly-trees from statistical data," in [*Proceedings of the Uncertainty in Artificial Intelligence 3 Annual Conference on Uncertainty in Artificial Intelligence (UAI-87)*], 0–0, Elsevier Science, Amsterdam, NL (1987).

[17] Lilliefors, H., "On the kolmogorov-smirnov test for normality with mean and variance unknown," *Journal of the American Statistical Association* **62**, 399–402 (1967).

[18] Bollen, K. and Kline, R., "Structural Equations with Latent Variables," *Measurement* **14**, 16.

[19] Bollen, K., [*Structural equations with latent variables*], Wiley (1989).

[20] Kaplan, D., [*Structural equation modeling: Foundations and extensions*], SAGE Publications Inc (2008).

[21] Hu, L. and Bentler, P., "Fit indices in covariance structure modeling: Sensitivity to underparameterized model misspecification," *Psychological methods* **3**, 424–453 (1998).

[22] Scheines, R., Spirtes, P., Glymour, C., and Meek, C., "Tetrad II: Tools for discovery," (1994).

[23] Spirtes, P., Glymour, C., and Scheines, R., [*Causation, Prediction, and Search, Second Edition (Adaptive Computation and Machine Learning)*], The MIT Press (2001).

[24] Spirtes, P. and Glymour, C., "An Algorithm for Fast Recovery of Sparse Causal Graphs," *Social Science Computer Review* **9**(1), 62–72 (1991).

[25] Scheines, R., Hoijtink, H., and Boomsma, A., "Bayesian estimation and testing of structural equation models," *Psychometrika* **64**(1), 37–52 (1999).